Nonlinear Dyn (2017) 90:765–779
DOI 10.1007/s11071-017-3609-8

ORIGINAL PAPER

On the dynamics of a spinning top under high-frequency excitation: part I—pivot point under vertical harmonic vibration

Hiba Sheheitli

Received: 20 January 2017 / Accepted: 8 June 2017 / Published online: 19 September 2017

Abstract We investigate the dynamics of a spinning top whose pivot point undergoes a small amplitude high-frequency vertical vibration. The method of Direct Partition of Motion is used to obtain an autonomous equation governing the leading order slow dynamics of the top's nutation and to derive an approximate closed form solution for the forced spinning top problem. We show that the fast vibration can lead to the stabilization of the "sleeping top" state and an expression for the minimum amplitude required is given in terms of system parameters. We also show the existence of a degenerate family of special solutions in which the spinning top is locked at constant nutation and precession angles; we refer to those as "skewed sleeping top" states. We derive the conditions under which these states exist and are stable. The results are verified through numerical integration of the full non-autonomous system.

Keywords Spinning top · High-frequency excitation · Stabilization · Bifurcation

H. Sheheitli (✉)
Department of Industrial and Mechanical Engineering, Lebanese American University, Byblos, Lebanon
e-mail: hiba.sheheitli@lau.edu.lb

1 Introduction

The spinning top is a classic paradigm for illustrating gyroscopic effects, the understanding of which is essential for numerous technological applications such as inertial sensors for navigation [6], spacecraft attitude control [8] and gyroscopic wave energy harvesting [12]. A heavy gyroscope with harmonic excitation has been studied in [3]; however, the excitation frequencies considered were of $O(1)$ and $O(\varepsilon)$, i.e., the effect of a high-frequency excitation was not considered. The non-trivial effects of high-frequency excitation on various nonlinear mechanical systems have been extensively studied and reviewed in recent years [2,5,11]. Such effects include changes in the number of equilibrium points, stability of equilibrium points, natural frequencies, stiffness and bifurcation paths. The most famous non-trivial effect of fast excitation is the stabilization of the pendulum in the upright position when its point of support is subjected to an imperceptible but very fast vertical oscillation. The method of Direct Partition of Motion (DPM) [2] has proved to be an efficient and powerful analytical method for the study of nonlinear systems under high-frequency excitation. The use of this method here allows us to obtain a closed form approximate solution to the spinning top under the influence of fast vibration. In 1908, Stephenson suggested that the unstable position of upright equilibrium for a symmetrical top may be rendered stable by an imposed fast vertical vibration of the point of support [9]. In addition to validating Stephenson's suggestion,

we here show that for special parameter values, a whole family of unexpected degenerate stable solutions exist in which the spinning top is locked at a nonzero nutation angle from the vertical position, without any precessional motion. For the best of our knowledge, this non-trivial effect has not been previously reported in the literature.

In Sect. 2, we derive the equations of motion for the system and apply DPM to obtain an autonomous second-order equation governing the leading order slow dynamics of the top's nutation. In Sect. 3, we study the stability of the classical "sleeping top" state in addition to the existence and stability of the non-trivial "skewed sleeping top" solutions. We then show that the equation for the leading order nutation angle possesses an exact closed form solution expressed in terms of the Jacobi elliptic functions. In Sect. 4, we present a numerical check of the results and compare the approximate solution to the exact solution obtained from the numerical integration of the full non-autonomous system.

2 The equations of motion

Consider a top of mass M, whose pivot point has a vertical position $z\,(t)$ from a fixed reference point. The center of mass (G) of the top is at a distance d from the pivot point, along the long axis of the top (see figure 5.7 in [4]).

2.1 The Lagrangian

We follow the classical mechanics approach for obtaining the rigid body equations of motion [4]. The position vector of points on the body can be written as: $\mathbf{r}_i = z\hat{k} + \mathbf{R}_i$ where $\hat{i}, \hat{j}, \hat{k}$ are orthonormal unit vectors in the inertial frame of reference.

The kinetic energy of the turning top is given by $T = \frac{1}{2}\int (v_i)^2\,\mathrm{d}m$, where

$$\mathbf{v}_i = \frac{\mathrm{d}\mathbf{r}_i}{\mathrm{d}t} = \dot{z}\hat{k} + \frac{\mathrm{d}\mathbf{R}_i}{\mathrm{d}t} = \dot{z}\hat{k} + \boldsymbol{\omega}\times\mathbf{R}_i$$

and the integral is over the whole volume of the body. The angular velocity vector of the top, $\boldsymbol{\omega}$, can be written in terms of the Euler angles (ϕ, θ, ψ) and their derivatives:

$$\boldsymbol{\omega} = \omega_1\hat{b}_1 + \omega_2\hat{b}_2 + \omega_3\hat{b}_3$$

$$\text{with}\quad \begin{cases} \omega_1 = \dot{\phi}\sin\theta\sin\psi + \dot{\theta}\cos\psi \\ \omega_2 = \dot{\phi}\sin\theta\cos\psi - \dot{\theta}\sin\psi \\ \omega_3 = \dot{\phi}\cos\theta + \dot{\psi} \end{cases}$$

The Euler angles used here are those defined in figure 4.7 in [4]. Also $\hat{b}_1$, $\hat{b}_2$, $\hat{b}_3$ are orthonormal unit vectors along x',y',z', respectively, that is, along the axis of the body frame of reference depicted in the aforementioned figure.

Expanding the expression for the kinetic energy:

$$T = \frac{1}{2}\int \Big[\dot{z}\hat{k}\cdot\dot{z}\hat{k} + 2\dot{z}\hat{k}\cdot(\boldsymbol{\omega}\times\mathbf{R}_i) + (\boldsymbol{\omega}\times\mathbf{R}_i)\cdot(\boldsymbol{\omega}\times\mathbf{R}_i)\Big]\,\mathrm{d}m$$

We have:

$$(\boldsymbol{\omega}\times\mathbf{R}_i)\cdot(\boldsymbol{\omega}\times\mathbf{R}_i) = \boldsymbol{\omega}\cdot(\mathbf{R}_i\times\boldsymbol{\omega}\times\mathbf{R}_i)$$

so

$$T = \frac{1}{2}M\,(\dot{z})^2 + \dot{z}\hat{k}\cdot\left(\boldsymbol{\omega}\times\int\mathbf{R}_i\,\mathrm{d}m\right) + \frac{1}{2}\boldsymbol{\omega}\cdot\left(\int\mathbf{R}_i\times\boldsymbol{\omega}\times\mathbf{R}_i\,\mathrm{d}m\right)$$

also

$$\int\mathbf{R}_i\,\mathrm{d}m = M d\hat{b}_3\ \&\ \int\mathbf{R}_i\times\boldsymbol{\omega}\times\mathbf{R}_i\,\mathrm{d}m = \mathbf{L} = \bar{I}\boldsymbol{\omega}$$

$\mathbf{L}$ and $\bar{I}$ denote the angular momentum vector and the moment of inertia tensor of the top about its pivot point, respectively. The simplified kinetic energy expression becomes:

$$T = \frac{1}{2}M\,(\dot{z})^2 + \dot{z}\hat{k}\cdot\left(\boldsymbol{\omega}\times M d\hat{b}_3\right) + \frac{1}{2}\boldsymbol{\omega}\bar{I}\boldsymbol{\omega} \qquad (1)$$

The third term on the right-hand side of Eq. (1) reduces to:

$$\frac{1}{2}\boldsymbol{\omega}\bar{I}\boldsymbol{\omega} = \frac{1}{2}\left(I_1\omega_1^2 + I_2\omega_2^2 + I_3\omega_3^2\right)$$

where I_1, I_2 and I_3 are the principal moments of inertia of the top. Assuming $I_1 = I_2$, we get:

$$\frac{1}{2}\boldsymbol{\omega}\bar{I}\boldsymbol{\omega} = \frac{1}{2}I_1\left(\dot{\phi}^2\sin^2\theta + \dot{\theta}^2\right) + \frac{1}{2}I_3\left(\dot{\phi}^2\cos^2\theta + \dot{\psi}^2\right) + I_3\dot{\phi}\dot{\psi}\cos\theta$$

We have $\hat{k} = (0, 0, 1)$ in the inertial frame of reference, and $\hat{b}_3 = (0, 0, 1)$ in the body frame of reference. To evaluate the second term of the right-hand side of Eq. (1), we make use of the following linear transformation from the inertial frame of reference to the body frame of reference: (c ≡ cos, s ≡ sin)

$$A = \begin{bmatrix} \mathrm{c}\psi\mathrm{c}\phi - \mathrm{c}\theta\mathrm{s}\phi\mathrm{s}\psi & \mathrm{c}\psi\mathrm{s}\phi + \mathrm{c}\theta\mathrm{c}\phi\mathrm{s}\psi & \mathrm{s}\psi\mathrm{s}\theta \\ -\mathrm{s}\psi\mathrm{c}\phi - \mathrm{c}\theta\mathrm{s}\phi\mathrm{c}\psi & -\mathrm{s}\psi\mathrm{s}\phi + \mathrm{c}\theta\mathrm{c}\phi\mathrm{c}\psi & \mathrm{c}\psi\mathrm{s}\theta \\ \mathrm{s}\theta\mathrm{s}\phi & -\mathrm{s}\theta\mathrm{c}\phi & \mathrm{c}\theta \end{bmatrix}$$

After algebraic manipulation, the full expression for the kinetic energy of the top becomes:

$$T = \frac{1}{2}M\left(\dot{z}\right)^2 + Md\dot{z}\dot{\theta}\sin\theta + \frac{1}{2}I_1\left(\dot{\phi}^2\sin^2\theta + \dot{\theta}^2\right) + \frac{1}{2}I_3\left(\dot{\phi}^2\cos^2\theta + \dot{\psi}^2\right) + I_3\dot{\phi}\dot{\psi}\cos\theta \quad (2)$$

The gravitational potential energy of the top is $V = Mgd\cos\theta$. So the Lagrangian is:

$$\begin{aligned} L &= T - V \\ &= \frac{1}{2}M\left(\dot{z}\right)^2 + Md\dot{z}\dot{\theta}\sin\theta + \frac{1}{2}I_1\left(\dot{\phi}^2\sin^2\theta + \dot{\theta}^2\right) \\ &\quad + \frac{1}{2}I_3\left(\dot{\phi}^2\cos^2\theta + \dot{\psi}^2\right) \\ &\quad + I_3\dot{\phi}\dot{\psi}\cos\theta - Mgd\cos\theta \end{aligned} \quad (3)$$

As a quick check, it can be seen that setting $\dot{z} = 0$ in Eq. (3) leads to the expression for the Lagrangian of the classical spinning top with a fixed pivot (eq.(5.52) in [4])

2.2 Hamilton's equations

The generalized momenta corresponding to ϕ, θ and ψ, respectively, are:

$$\begin{aligned} p_\phi &= \frac{\partial L}{\partial\dot{\phi}} = \dot{\phi}\left(I_1\sin^2\theta + I_3\cos^2\theta\right) + I_3\dot{\psi}\cos\theta \\ p_\theta &= \frac{\partial L}{\partial\dot{\theta}} = Md\dot{z}\sin\theta + I_1\dot{\theta} \\ p_\psi &= \frac{\partial L}{\partial\dot{\psi}} = I_3\dot{\phi}\cos\theta + I_3\dot{\psi} \end{aligned} \quad (4)$$

From Eq. (4), we obtain expressions for $\dot{\phi}, \dot{\theta}$ and $\dot{\psi}$ in terms of p_ϕ, p_θ and p_ψ:

$$\begin{aligned} \dot{\theta} &= \frac{1}{I_1}\left(p_\theta - Md\dot{z}\sin\theta\right) \\ \dot{\phi} &= \frac{1}{I_1\sin^2\theta}\left(p_\phi - p_\psi\cos\theta\right) \\ \dot{\psi} &= \frac{\cos\theta}{I_1\sin^2\theta}\left(p_\psi\cos\theta - p_\phi\right) + \frac{p_\psi}{I_3} \end{aligned} \quad (5)$$

The Hamiltonian is then given by:

$$\begin{aligned} H &= \dot{\phi}p_\phi + \dot{\theta}p_\theta + \dot{\psi}p_\psi - L \\ &= \frac{1}{2I_1\sin^2\theta}p_\phi^2 + \frac{1}{2I_1}p_\theta^2 + \frac{1}{2}\left(\frac{1}{I_3} + \frac{\cos^2\theta}{I_1\sin^2\theta}\right)p_\psi^2 \\ &\quad - \frac{\cos\theta}{I_1\sin^2\theta}p_\psi p_\phi - \frac{Md}{I_1}\dot{z}p_\theta\sin\theta - \frac{1}{2}M\left(\dot{z}\right)^2 \\ &\quad + \frac{M^2d^2}{2I_1}\left(\dot{z}\right)^2\sin^2\theta + Mgd\cos\theta \end{aligned} \quad (6)$$

We can see that ϕ and ψ are cyclic coordinates; hence, p_ϕ and p_ψ are conserved and the dynamics reduces to a one degree of freedom system governing the nutation angle θ. That is, p_ϕ and p_ψ act as parameters for the nutation dynamics. The Hamilton's equations for θ are:

$$\begin{aligned} \dot{\theta} &= \frac{1}{I_1}\left(p_\theta - Md\dot{z}\sin\theta\right) \\ \dot{p}_\theta &= \frac{p_\psi}{I_1\sin\theta}\left(p_\psi\cos\theta - p_\phi\right) \\ &\quad + \frac{\cos\theta}{I_1\sin^3\theta}\left(p_\psi\cos\theta - p_\phi\right)^2 \\ &\quad + Mgd\sin\theta + \frac{Md}{I_1}\dot{z}p_\theta\cos\theta \\ &\quad - \frac{M^2d^2}{I_1}\left(\dot{z}\right)^2\sin\theta\cos\theta \end{aligned}$$

Then the resulting second-order equation on θ is given by:

$$\begin{aligned} &\ddot{\theta} - \frac{p_\psi}{I_1^2\sin\theta}\left(p_\psi\cos\theta - p_\phi\right) \\ &- \frac{\cos\theta}{I_1^2\sin^3\theta}\left(p_\psi\cos\theta - p_\phi\right)^2 \\ &- \frac{Md}{I_1}\left(g - \ddot{z}\right)\sin\theta = 0 \end{aligned} \quad (7)$$

2.3 The method of direct partition of motion

We consider the vibration of the pivot point to be of a very small amplitude but very large frequency, that is, $z\left(t\right) = A\cos\left(\omega t\right)$ with $A = O\left(\varepsilon\right)$ and $\omega = \frac{1}{\varepsilon}$ where $\varepsilon << 1$. Then $\ddot{z}\left(t\right) = -A\omega^2\cos\left(\omega t\right) = -a\omega\cos\left(\omega t\right)$ where $a = A\omega = O\left(1\right)$

We define two main timescales: the slow timescale t and the fast timescale $\tau = \omega t = \frac{t}{\varepsilon}$. DPM is based on three main assumptions [2]:

- the motion of the system under fast excitation can be partitioned into a purely slow component and an overlaid fast component.
- any function of fast time is periodic with a zero average over a period of fast time.
- any purely slow function is invariant under averaging over fast time. That is, t is considered a constant when integrating with respect to τ.

We start with the first basic ansatz of DPM and decompose the solution to Eq. (7) into a leading order slow

component, θ_0, and a small overlaid fast component, $\epsilon\theta_1$, i.e.,

$$\theta = \theta_0(t) + \varepsilon\theta_1(t,\tau) \tag{8}$$

According to the second and third ansatzs, θ_1 is assumed periodic in τ with a zero average over one period of fast time, while the slow component, θ_0, remains unchanged under the later operation, that is:

$$\theta_1(\tau+2\pi) = \theta_1(\tau), \quad \langle\theta_1\rangle_\tau = 0, \quad \langle\theta_0\rangle_\tau = \theta_0$$

$$\text{where} \qquad \langle\cdot\rangle_\tau = \frac{1}{2\pi}\int_0^{2\pi}\cdot\,\mathrm{d}\tau$$

These conditions on θ_1 also apply to all of its derivatives, and the same is true for θ_0. To implement the DPM procedure, we differentiate Eq. (8) with respect to t:

$$\ddot{\theta} = \frac{\mathrm{d}^2\theta_0}{\mathrm{d}t^2} + 2\frac{\partial^2\theta_1}{\partial t\partial\tau} + \varepsilon\frac{\partial^2\theta_1}{\partial t^2} + \frac{1}{\varepsilon}\frac{\partial^2\theta_1}{\partial\tau^2}$$

We plug this into Eq. (7) along with Eq. (8) and expand the nonlinear terms into a Taylor series about $\epsilon = 0$. Collecting terms of the same order in ϵ, we obtain the following equations governing θ_1 and θ_0:

$$O\left(\frac{1}{\varepsilon}\right): \quad \frac{\partial^2\theta_1}{\partial\tau^2} = \frac{Mda}{I_1}\cos\tau\sin\theta_0 \tag{9}$$

$$\begin{aligned} O(1): \quad & \frac{\mathrm{d}^2\theta_0}{\mathrm{d}t^2} - \frac{p_\psi}{I_1^2\sin\theta_0}\left(p_\psi\cos\theta_0 - p_\phi\right) \\ & - \frac{\cos\theta_0}{I_1^2\sin^3\theta_0}\left(p_\psi\cos\theta_0 - p_\phi\right)^2 \\ & - \frac{Mdg}{I_1}\sin\theta_0 - \frac{Mda}{I_1}\theta_1\cos\tau\cos\theta_0 + 2\frac{\partial^2\theta_1}{\partial t\partial\tau} = 0 \end{aligned} \tag{10}$$

We integrate Eq. (9) twice with respect to τ to obtain:

$$\theta_1 = -\frac{Mda}{I_1}\cos\tau\sin\theta_0 + c_1\tau + c_2$$

By the second assumption of DPM, the two integration constants c_1 and c_2 have to be zero. So the expression for the fast component of motion reduces to:

$$\theta_1 = -\frac{Mda}{I_1}\cos\tau\sin\theta_0 \tag{11}$$

We insert this into Eq. (10):

$$\begin{aligned} & \frac{\mathrm{d}^2\theta_0}{\mathrm{d}t^2} - \frac{p_\psi}{I_1^2\sin\theta_0}\left(p_\psi\cos\theta_0 - p_\phi\right) \\ & - \frac{\cos\theta_0}{I_1^2\sin^3\theta_0}\left(p_\psi\cos\theta_0 - p_\phi\right)^2 \\ & - \frac{Mdg}{I_1}\sin\theta_0 + \left(\frac{Mda}{I_1}\right)^2\cos^2\tau\sin\theta_0\cos\theta_0 \\ & + 2\frac{Mda}{I_1}\sin\tau\cos\theta_0\frac{\mathrm{d}\theta_0}{\mathrm{d}t} = 0 \end{aligned}$$

To complete the DPM procedure, we average this equation over a period of fast time with the assumption that any purely slow function remains unchanged under this operation. The result is an autonomous equation that governs the leading order nutation motion of the spinning top:

$$\begin{aligned} & \frac{\mathrm{d}^2\theta_0}{\mathrm{d}t^2} - \frac{p_\psi}{I_1^2\sin\theta_0}\left(p_\psi\cos\theta_0 - p_\phi\right) - \frac{Mdg}{I_1}\sin\theta_0 \\ & - \frac{\cos\theta_0}{I_1^2\sin^3\theta_0}\left(p_\psi\cos\theta_0 - p_\phi\right)^2 \\ & + \frac{1}{2}\left(\frac{Mda}{I_1}\right)^2\sin\theta_0\cos\theta_0 = 0 \end{aligned} \tag{12}$$

3 Leading order nutation dynamics

3.1 Stabilization of the "sleeping top"

The classical spinning top possesses an equilibrium point at $\theta = 0$, referred to as the "sleeping top" state [1], which is known to be stable for:

$$p_\psi \geq 2\sqrt{MgdI_1} \tag{13}$$

The naming of this state is due to the fact that when dissipation is present, a "sleeping top" spinning at $\theta = 0$ is seen to "awaken" as p_ψ decreases and the upright position looses stability. Due to the particular choice of the Euler angles as coordinates, the equation governing θ_0 is singular at 0 and π which correspond to the upright and downwards equilibrium positions of the spinning top, respectively. To study the stability of the latter states, we observe that the nutation dynamics described by Eq. (12) can be seen as a one degree of freedom system driven by the following effective potential function:

$$\begin{aligned} U_{\text{eff}} = & \frac{\left(p_\phi - p_\psi\cos\theta_0\right)^2}{2I_1\sin^2\theta_0} + Mgd\cos\theta_0 \\ & - \frac{(Mda)^2}{4I_1}\cos^2\theta_0 \end{aligned} \tag{14}$$

We expand this potential function in a Taylor series about $\theta_0 = 0$ with the condition $p_\phi = p_\psi$ which

follows from evaluating the expressions in Eq. (4) at $\theta = 0$. We get:

$$U_{\text{eff}} = c_1 + c_2\theta_0^2 + \cdots$$

$$\text{where} \quad c_1 = Mgd - \frac{(Mda)^2}{4I_1}$$

$$\& \quad c_2 = \frac{p_\psi^2}{8I_1} + \frac{(Mda)^2}{4I_1} - \frac{1}{2}Mgd$$

We can deduce that the upright position if stable when $c_2 > 0$, that is, when:

$$a > \sqrt{\frac{2gI_1}{Md} - \frac{p_\psi^2}{2M^2d^2}} \quad \text{i.e.,}$$

$$p_\psi > \sqrt{4MgdI_1 - 2M^2d^2a^2} \tag{15}$$

Note that for $a = 0$, this condition reduces to Eq. (13), the already known condition for the unforced top. Next, expanding the effective potential function about $\theta_0 = \pi$ with the condition $p_\phi = -p_\psi$, we obtain:

$$U_{\text{eff}} = c_1 + c_2\,(\theta_0 - \pi)^2 + \cdots$$

$$\text{where} \quad c_1 = -Mgd - \frac{(Mda)^2}{4I_1}$$

$$\& \quad c_2 = \frac{p_\psi^2}{8I_1} + \frac{(Mda)^2}{4I_1} + \frac{1}{2}Mgd$$

$c_2 > 0$, i.e., the downwards state is stable for all values of a and p_ψ.

3.2 Non-trivial solutions: "skewed sleeping top" states

To investigate the existence of non-trivial equilibrium states for the leading order nutation dynamics, we look for equilibrium points, other than $\theta = 0$ and $\theta = \pi$. Such states will correspond to $\frac{\mathrm{d}^2\theta_0}{\mathrm{d}t^2} = 0$ and $\frac{\mathrm{d}\theta_0}{\mathrm{d}t} = 0$, i.e., to values of θ_0 that satisfy the following algebraic equation:

$$p_\psi\left(p_\psi\cos\theta_0 - p_\phi\right)\sin^2\theta_0 + \cos\theta_0\left(p_\psi\cos\theta_0 - p_\phi\right)^2 + MgdI_1\sin^4\theta_0 - \frac{1}{2}(Mda)^2\sin^4\theta_0\cos\theta_0 = 0 \tag{16}$$

For the spinning top to be in a "skewed sleeping top" state, that is, to keep a constant nutation angle $\theta_0 = \theta_0^*$ without precessing, its rate of precession $\dot{\phi}$ needs to be zero for all time. From Eq. (5), this leads to the following condition on the parameters p_ϕ and p_ψ:

$$p_\phi = p_\psi\cos\theta_0^* \tag{17}$$

Plugging this into Eq. (16), we obtain an expression for the nutation angle corresponding to the skewed sleeping top state:

$$\theta_0^* = \cos^{-1}\left(\frac{2gI_1}{Mda^2}\right) \tag{18}$$

It follows that such states exist for:

$$a > \sqrt{\frac{2gI_1}{Md}} \tag{19}$$

To study the stability of the skewed sleeping top state, we linearize the system governing θ_0 and evaluate its Jacobian at $\theta_0 = \theta_0^*$, $\frac{\mathrm{d}\theta_0}{\mathrm{d}t} = 0$ with $p_\phi = p_\psi\cos\theta_0^*$, to get:

$$J = \begin{bmatrix} 0 & 1 \\ -\frac{p_\psi^2}{I_1^2} + \frac{(Mda)^2}{2I_1^2} - \frac{2g^2}{a^2} & 0 \end{bmatrix}$$

The corresponding eigenvalues have the following expression:

$$\lambda_{1,2} = \pm\frac{\sqrt{a^4d^2M^2 - 2a^2p_\psi^2 - 4g^2I_1^2}}{\sqrt{2}aI_1}$$

We examine the function that is under the square root:

$$f = a^4d^2M^2 - 2a^2p_\psi^2 - 4g^2I_1^2$$

This is a quadratic function in a^2 with a positive coefficient of a^4 and has a minimum value of:

$$f_{\text{min}} = -\frac{p_\psi^4}{M^2d^2} - 4g^2I_1^2 \;<\; 0$$

with two possible roots that correspond to:

$$a_{1,2} = \sqrt{\frac{\pm\sqrt{p_\psi^4 + 4M^2g^2d^2I_1^2} + p_\psi^2}{M^2d^2}}$$

This means that $f < 0$ for $\mathrm{a}_2 < \mathrm{a} < \mathrm{a}_1$, and consequently, the eigenvalues are pure imaginary for these values of a. We thus conclude that the skewed sleeping top states exist and are stable when the following condition is satisfied:

$$\sqrt{\frac{2gI_1}{Md}} < \mathrm{a} < \sqrt{\frac{p_\psi^2 + \sqrt{p_\psi^4 + 4M^2g^2d^2I_1^2}}{M^2d^2}} \tag{20}$$

In summary, the analysis predicts that the spinning top, under the influence of the fast vertical vibration, will behave as if it had an apparent equilibrium state described by ($\theta = \theta_0^*$, $\dot{\phi} = 0$), when the parameters are chosen to satisfy conditions in Eqs. (17) and (20).

3.3 Exact solution for the leading order nutation

We observe that Eq. (12) governing θ_0 represents a one degree of freedom system with an effective total energy function given by:

$$\bar{E} = \frac{1}{2} I_1 \dot{\theta}_0^2 + U_{\text{eff}}$$
$$= \frac{1}{2} I_1 \dot{\theta}_0^2 + \frac{\left(p_\phi - p_\psi \cos\theta_0\right)^2}{2 I_1 \sin^2\theta_0}$$
$$+ Mgd\cos\theta_0 - \frac{(Mda)^2}{4 I_1}\cos^2\theta_0$$

which can be written as:

$$E = \dot{\theta}_0^2 + \frac{(\eta - \kappa\cos\theta_0)^2}{\sin^2\theta_0} + \nu\cos\theta_0 - \rho\cos^2\theta_0$$

where $\eta = \frac{p_\phi}{I_1}$, $\kappa = \frac{p_\psi}{I_1}$, $\nu = \frac{2Mgd}{I_1}$, $\rho = \frac{1}{2}\left(\frac{Mda}{I_1}\right)$

We define the new variable $u = \cos\theta_0$, then the above expression for E can be rewritten as:

$$E = \dot{u}^2 + \rho u^4 - \nu u^3 + \left(E + \kappa^2 - \rho\right) u^2$$
$$+ (\nu - 2\eta\kappa)\, u + \eta^2,$$

i.e., it is of the form:

$$E = \dot{u}^2 + V(u)$$
where $V(u) = A_1 + B_1 u + C_1 u^2 + D_1 u^3 + F_1 u^4$
with $A_1 = \eta^2$, $B_1 = \nu - 2\eta\kappa$, $C_1 = E + \kappa^2 - \rho$
$D_1 = -\nu$, $F_1 = \rho$

This represents an anharmonic quartic potential oscillator, for which the exact solution is given in terms of the Jacobi elliptic functions [7]. We first translate the system coordinate to u_0 which is a local minimum of the potential function $V(u)$. u_0 is the root of the first derivative of $V(u)$, i.e., the solution to:

$$B_1 + 2C_1 u + 3D_1 u^2 + 4F_1 u^3 = 0$$

If three real roots exist, $u_1 < u_2 < u_3$, then $u_0 = u_2$. With the new translated coordinate $x = u - u_0$, the energy expression becomes[7]:

$$E^* = \dot{x}^2 + Ax^2 + Bx^3 + Cx^4 \tag{21}$$

where $A = E + \kappa^2 - \rho - 3\nu u_0 + 6\rho u_0^2$, $B = -\nu + 4\rho u_0 C = \rho$, $E^* = E - \left(A_1 + B_1 u_0 + C_1 u_0^2 + D_1 u_0^3 + F_1 u_0^4\right)$.

Equation (21) is separable and leads to:

$$\left[E^* - Ax^2 - Bx^3 - Cx^4\right]^{-1/2} \mathrm{d}x = \mathrm{d}t$$

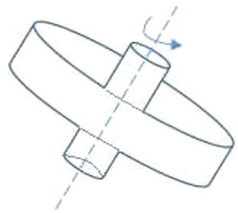

Fig. 1 Schematic of the shape of the spinning top

which we rewrite as:

$$[(x-a)(x-b)(x-c)(x-d)]^{-1/2}\,\mathrm{d}x = |C|^{1/2}\,\mathrm{d}t \tag{22}$$

where a, b, c and d are the roots of $Ax^2 + Bx^3 + Cx^4 = E^*$. The full details of the integration of Eq. (22) are given in [7] where it is reported that the general solution has the form:

$$x = \frac{\left[\alpha + \beta \mathrm{pq}^e(\omega t; m)\right]}{\left[\gamma + \delta \mathrm{pq}^e(\omega t; m)\right]} \tag{23}$$

pq represents one of the Jacobi elliptic functions, the choice of which, along with α,β,γ,δ and e, is specified in terms of a, b, c, d and the x range of interest. The reader is referred to [7] for the full details.

4 Numerical validation

Without loss of generality, we choose the spinning top to have the shape illustrated in Fig. 1, with a 4 kg disk of 1 m radius and 10 cm thickness, and a 0.8 kg rod with 20 cm radius and 50 cm length. This leads to the following values for the physical parameters: $I_1 = 1.438\,\mathrm{kg\,m^2}$, $I_3 = 2.016\,\mathrm{kg\,m^2}$, $d = 0.2917\,\mathrm{m}$, $\mathrm{M} = 4.8\,\mathrm{kg}$.

We start by validating the presence and stability of the "skewed sleeping top" states, and at the same time we compare the exact solution obtained by numerical integration of the full non-autonomous system to the approximate closed form solution that is given in Eqs. (8), (11) and (23). The initial condition specifies the choice of the Jacobi elliptic function and the values of the constants that appear in Eq. (23), as reported in the caption under each corresponding plot. For brevity, the algebraic details of the involved computations are not presented here as the process is fully detailed in [7].

In Fig. 2, we choose $p_\psi = 9$ for which the analysis predicts that the "skewed sleeping top" state exists and is stable for $4.49 \le a \le 9.34$. We take $a = 5$, which corresponds to $\theta_0^* = 0.633$ and a required value

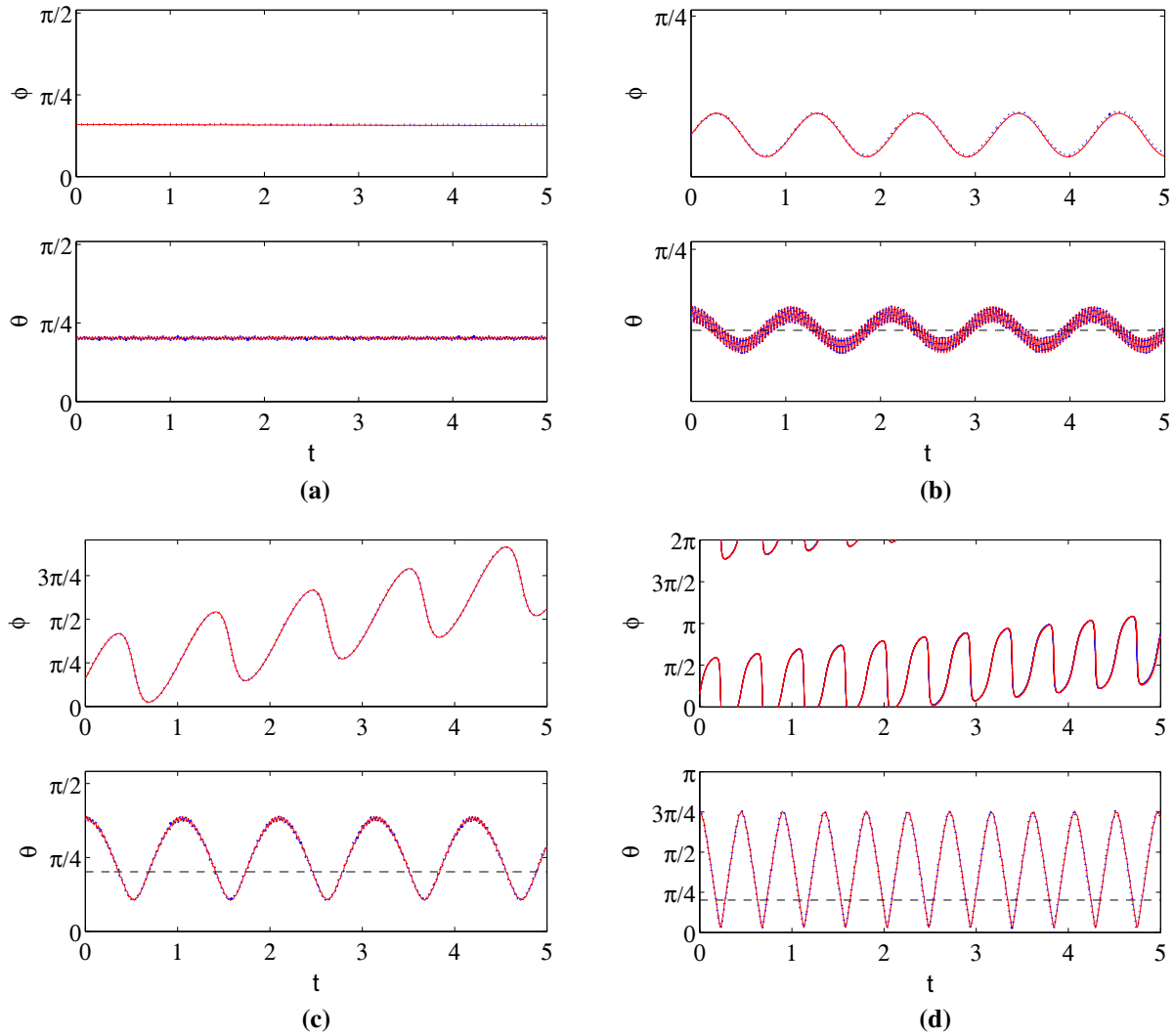

Fig. 2 Comparison of numerical integration solution (*red-solid line*) to the approximate closed form solution (*blue dotted line*) when the "skewed sleeping top" state is stable. Initial condition: $(\dot{\theta}(0) = 0, \dot{\phi}(0) = 0, \phi(0) = 0.5)$ and $\theta(0)$ as specified under each figure. parameter values: $p_\psi = 9$, $p_\phi = p_\psi \cos(\theta_0^*) = 7.255$, $a = 5$, $\epsilon = 0.005$ (*dotted black line* represents the value of θ_0^*). **a** $\theta(0) = 0.604$, $\theta_0(t) = \theta^* = 0.633$. **b** $\theta(0) = 0.648$; $pq \equiv cn, e = 1, \alpha = -5.6 \times 10^{-4}, \beta = -0.059$, $\gamma = 3.43, \delta = 0.016, w = 5.91, m = 7.9 \times 10^{-5}$. **c** $\theta(0) = 1.177$; $pq \equiv cn, e = 1, \alpha = -0.0099, \beta = -1.02, \gamma = 3.51, \delta = 0.16, w = 6.02, m = 0.025$. **d** $\theta(0) = 2.34$; $pq \equiv cn, e = 1, \alpha = 0.384, \beta = -6.96, \gamma = 8.17, \delta = -0.216, w = 14.05, m = 0.043$. (Color figure online)

of $p_\phi = p_\psi \cos(\theta_0^*) = 7.255$. The prediction is that for this choice of a and p_ϕ, if we start at the nutation angle corresponding to θ_0^* with any arbitrary initial ϕ value, the spinning top remains locked at its initial position while merely undergoing an $O(\epsilon)$ fast oscillation in its nutation angle. The plot in Fig. 2a confirms this prediction. To be more accurate, we point out that since the error in the approximate θ solution is of $O(\epsilon^2)$, then for the "skewed sleeping top" solutions $\dot{\phi} = 0 + O(\epsilon^2)$; this means that while the top practically appears to be locked without any precessional motion, it is actually drifting at an extremely slow rate.

We note that from Eqs. (8) and (11), it follows that for a desired initial θ_0 value, $\theta_0(0)$, the corresponding initial condition for θ is:

$$\theta\,(0) = \theta_0\,(0) - \epsilon \frac{Mda}{I_1} \sin\theta_0\,(0)$$

Figure 2b shows that if we start close enough to the "skewed sleeping top" state, the spinning top is locked to oscillate about its initial ϕ position. As the initial condition is chosen to be even farther from the θ_0^* state, the nutation oscillation grows bigger and more asymmetric (Fig. 2c, d) and the top drifts into a nonuniform precession.

It is worth noting that in all the shown results, the exact and approximate solutions almost entirely overlap and hence the subsequent Figs. 3 and 6 show a zoom in on the plots to make the comparison clearer. DPM assumes $\epsilon << 1$, so the smaller ϵ is, the greater is the validity of the approximate solution; Fig. 4 shows sample results for larger values of ϵ. While there is no exact cutoff for the required ϵ value, DPM assumes that $\epsilon\theta_1 = O(\epsilon)$ such that the amplitude $\epsilon \frac{Mda}{I_1} = O(\epsilon)$; hence, this sets a guide on how big ϵ can be for a chosen set of the physical parameters: M, d, a and I_1. For the values chosen here, $\epsilon = 0.02$ gives $\epsilon\theta_1$ an amplitude ≈ 0.21 which is

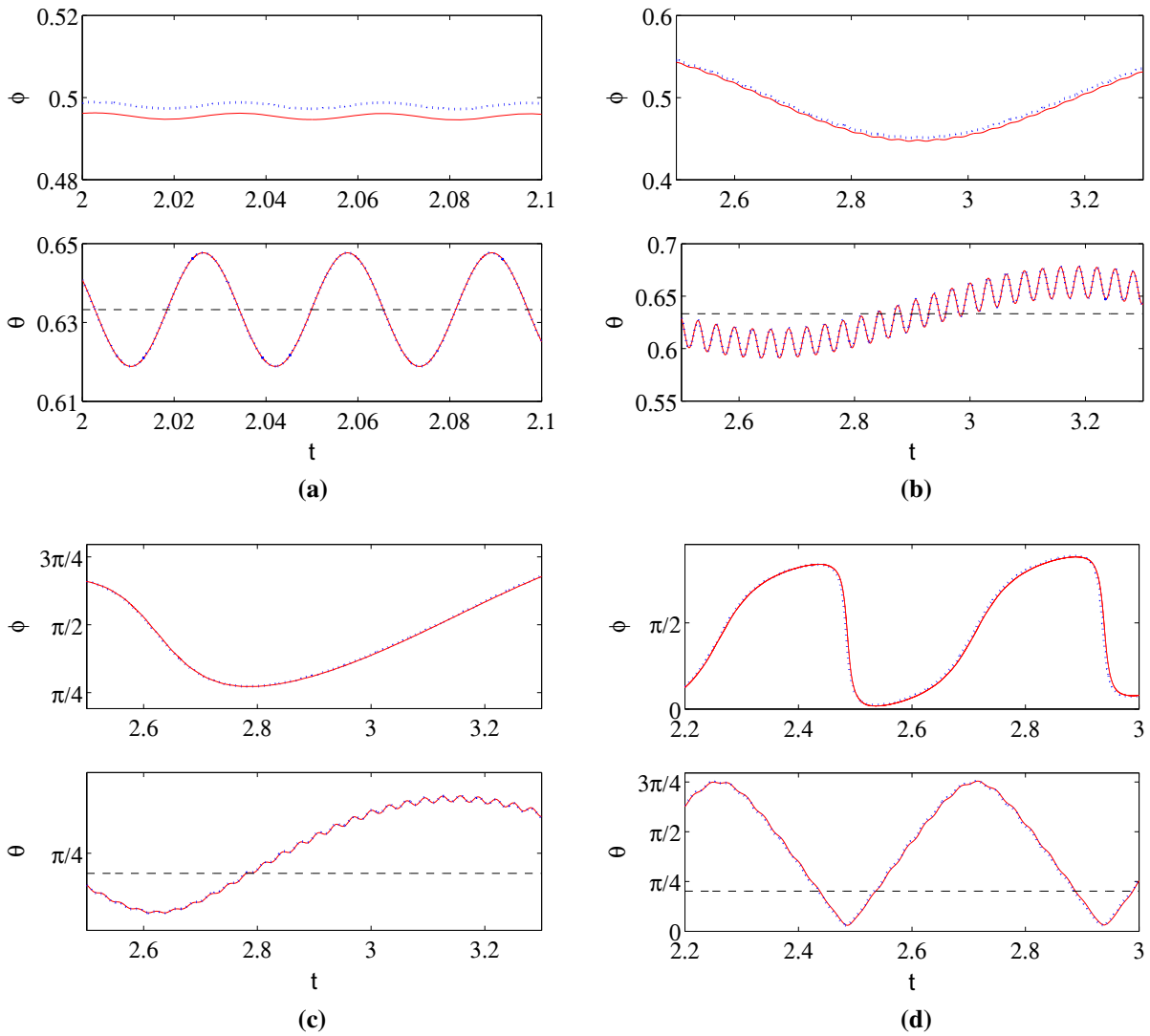

Fig. 3 Zoom in on solutions in Fig. 2. **a** Solution in Fig. 2a. **b** Solution in Fig. 2b. **c** Solution in Fig. 2c. **d** Solution in Fig. 2d. (Color figure online)

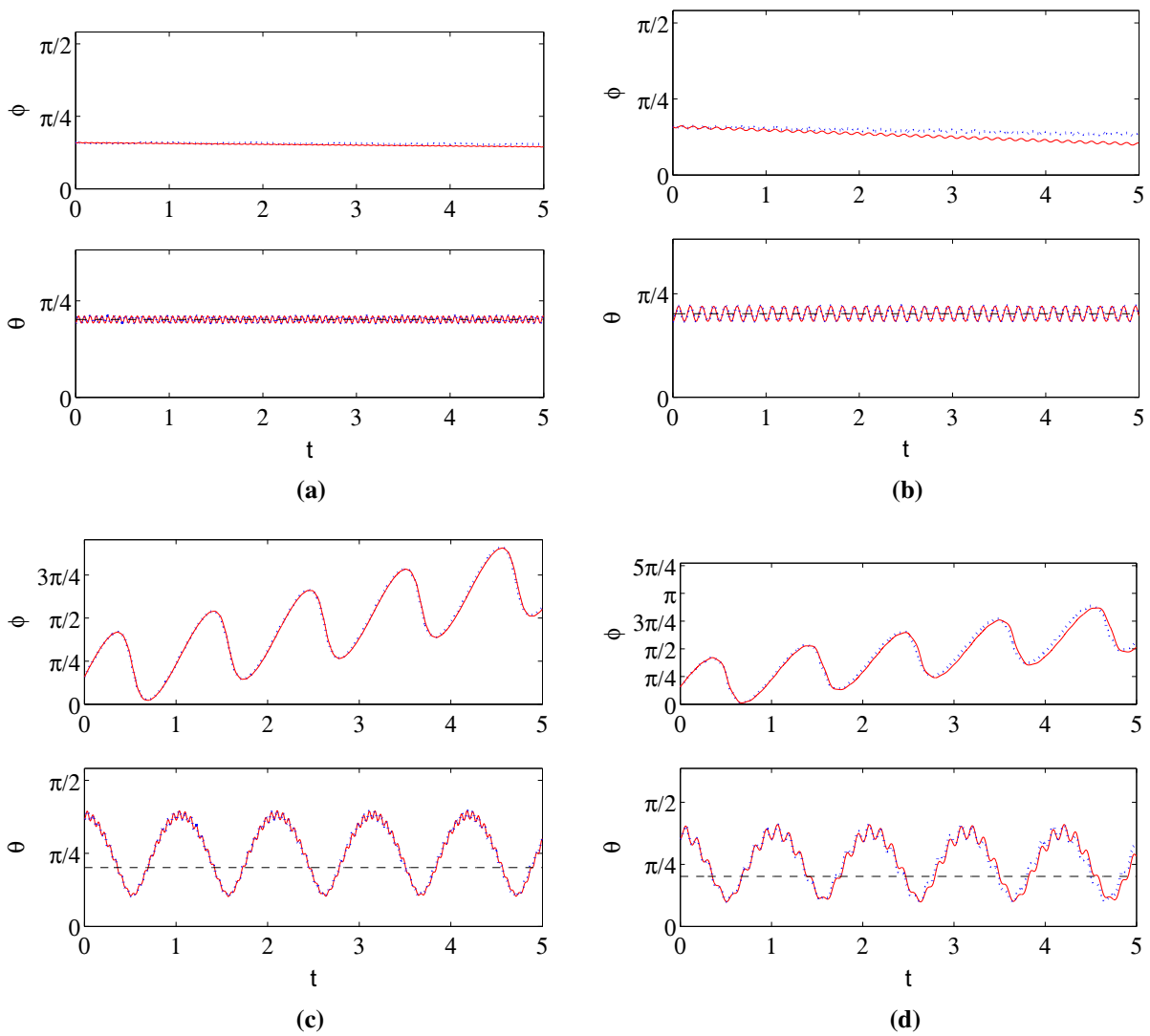

Fig. 4 As in Fig. 2, for different ϵ values. **a**, **b** correspond to starting at $\theta_0(0) = \theta_0^*$; **c**, **d** correspond to starting at $\theta_0(0) = 1.2$. **a** $\theta(0) = 0.604$, $\epsilon = 0.01$. **b** $\theta(0) = 0.575$, $\epsilon = 0.02$. **c** $\theta(0) = 1.154$, $\epsilon = 0.01$. **d** $\theta(0) = 1.109$, $\epsilon = 0.02$. (Color figure online)

close to $O(1)$; hence, the assumption breaks down and we see in Fig. 4b, d that the discrepancy between the exact solution and the predicted solution becomes more pronounced.

In Figs. 5 and 6, we also take $p_\psi = 9$ but with a=11 which corresponds to $\theta_0^* = 1.403$. With $p_\phi = p_\psi \cos\left(\theta_0^*\right) = 1.499$, the "skewed sleeping top" state exists but is unstable. Figure 7 shows the phase portrait for the θ_0 dynamics for the two sets of parameters used. While for $a = 5$, it is filled with closed orbits about the θ_0^* center, we can see that for $a = 11$, the θ_0^* state has lost stability through a pitchfork bifurcation. The two centers that emerge after the loss of stability correspond to uniform precession solutions in which θ_0 remains constant (Fig. 5c, d). Also, solutions starting close to θ_0^*, move away from it and instead oscillate about the uniform precession solutions (Fig. 5a, b).

We next look at the stability of the classical "sleeping top" state which corresponds to $\theta = 0$. For the chosen parameters, with $a = 0$, the "sleeping top" is stable for $p_\psi \geq 8.88$ (Eq. 13). We choose $p_\psi = 5$; then the analysis predicts that the high-frequency excitation stabilizes the "sleeping top" state when $a > 3.71$.

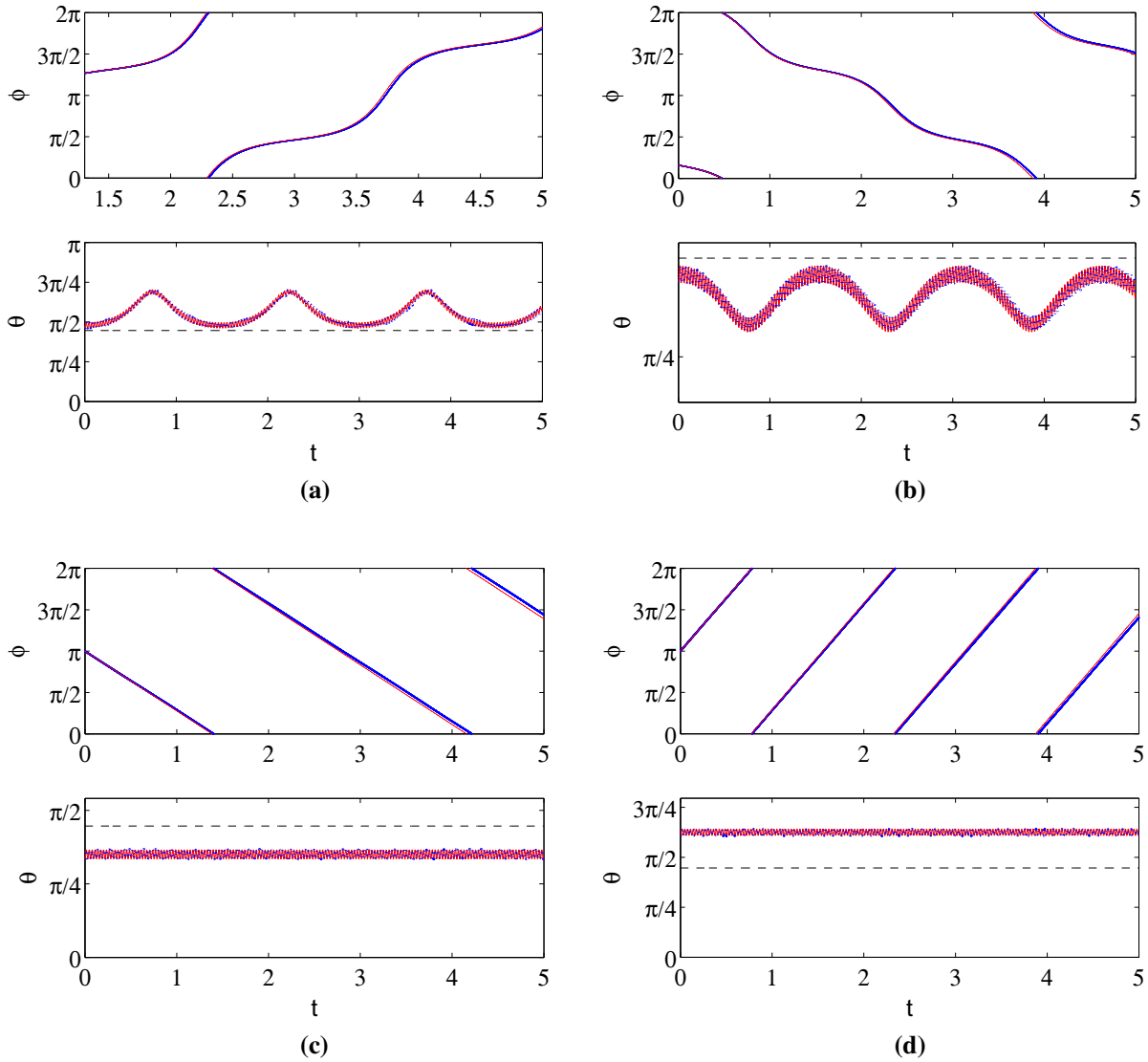

Fig. 5 As in Fig. 2, but with $p_\phi = p_\psi \cos\left(\theta_0^*\right) = 1.499$ and $a = 11$ for which the "skewed sleeping top" state is predicted to be unstable. **a** $\theta\,(0) = 1.45$; $pq \equiv sn, e = 2, \alpha = -0.349$, $\beta = 0.24, \gamma = 0.482, \delta = 0.627, w = 2.4, m = 0.427$ **b** $\theta\,(0) = 1.252$; $pq \equiv sn, e = 2, \alpha = 0.047, \beta = 0.0255$, $\gamma = 0.476, \delta = -0.288, w = 2.371, m = 0.468$. **c** $\theta\,(0) = 1.05$; $pq \equiv sn, e = 2, \alpha = 0.1397, \beta = 1.79 \times 10^{-4}, \gamma = 0.478, \delta = -9.73 \times 10^{-4}, w = 2.619, m = 1.06 \times 10^{-3}$. **d** $\theta\,(0) = 1.95$; $pq \equiv cn, e = 1, \alpha = -1.002, \beta = -2.68 \times 10^{-5}, \gamma = 1.917, \delta = -5.83 \times 10^{-5}, w = 7.26, m = 0$. (Color figure online)

Figures 8 and 9 confirm this; for a smaller than the critical value, solutions with initial θ values near 0 move away from it (Fig. 8a, b), however, as a is increased past the critical value, starting near 0 leads to oscillations about 0 (Fig. 9a, b). θ remains positive in these solutions since θ, as defined in the Euler angles coordinate system, has the range $[0,\pi]$. However physically, these latter oscillations correspond to the top oscillating about the upright "sleeping top" position and hence confirm its stability.

Interestingly, there exist values of p_ψ and a, for which both the classical "sleeping top" and the "skewed sleeping top" states are stable. In such a case, starting from the θ_0^* initial position could lead either to

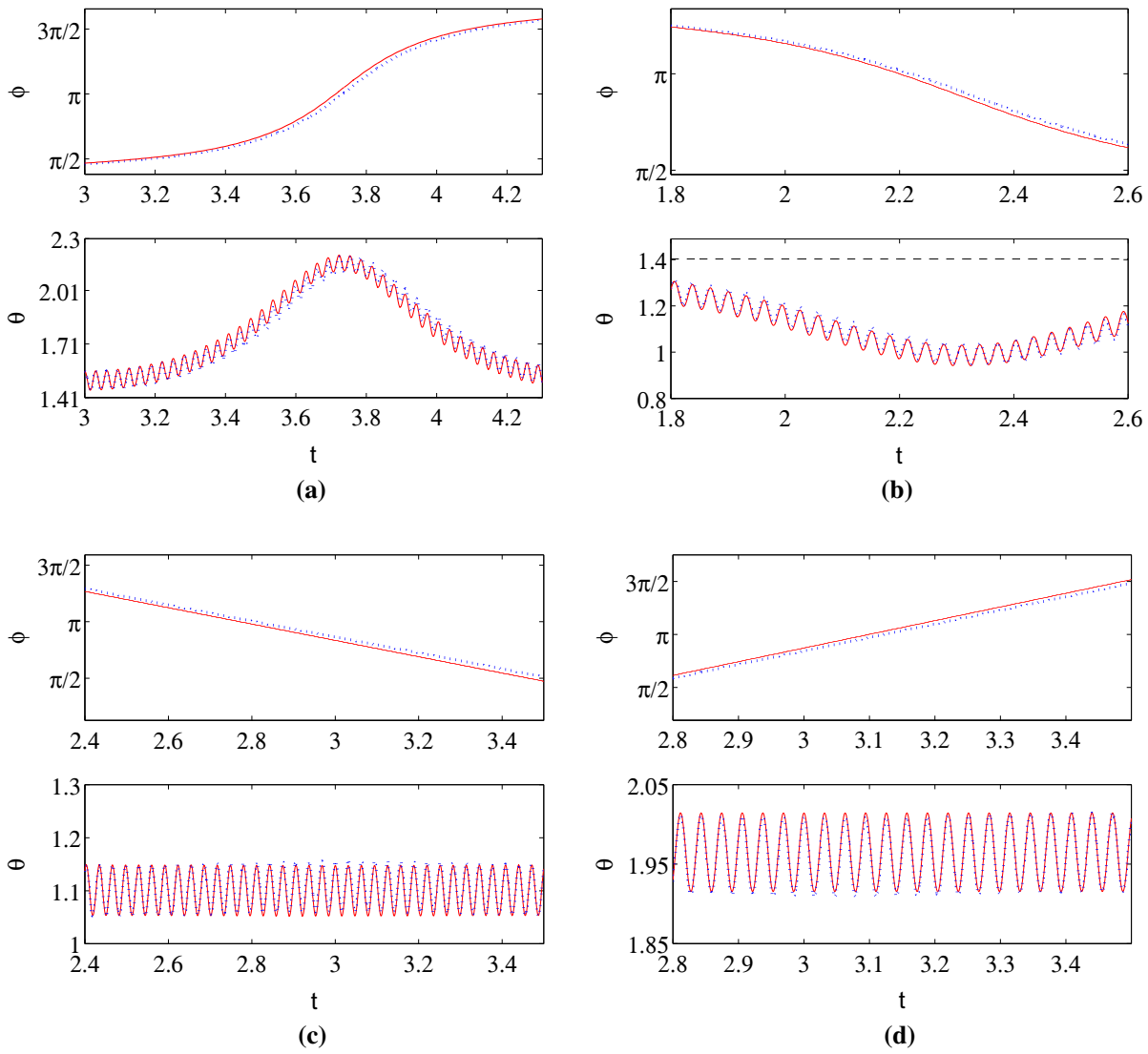

Fig. 6 Zoom in on solutions in Fig. 5. **a** Solution in Fig. 5a. **b** Solution in Fig. 5b. **c** Solution in Fig. 5c. **d** Solution in Fig. 5d. (Color figure online)

an oscillation about the upright "sleeping top" position (Fig. 10a) if $p_\phi = p_\psi$ or to being locked in the "skewed sleeping top" state if $p_\phi = p_\psi \cos\left(\theta_0^*\right)$ (Fig. 10b).

Finally, it is worth noting that the system studied here does not take into account any dissipative effects and so the apparent equilibrium states referred to here as stable are in fact only marginally stable, with purely imaginary eigenvalues. To check whether these states would persist to be asymptotically stable in the presence of dissipation, we perform a simple numerical test by adding linear viscous damping into the system. We assume a simple dissipation function of the form:

$$F = \frac{1}{2}\mu_\theta \dot{\theta}^2 + \frac{1}{2}\mu_\phi \dot{\phi}^2 + \frac{1}{2}\mu_\psi \dot{\psi}^2$$

The resulting Lagrange's equations governing the Euler angles of the spinning top become:

$$I_1\ddot{\theta} + (I_3 - I_1)\,\dot{\phi}^2 \cos\theta \sin\theta + I_3\dot{\psi}\dot{\phi}\sin\theta$$
$$-Md\,(g - \ddot{z})\sin\theta + \mu_\theta\dot{\theta} = 0$$

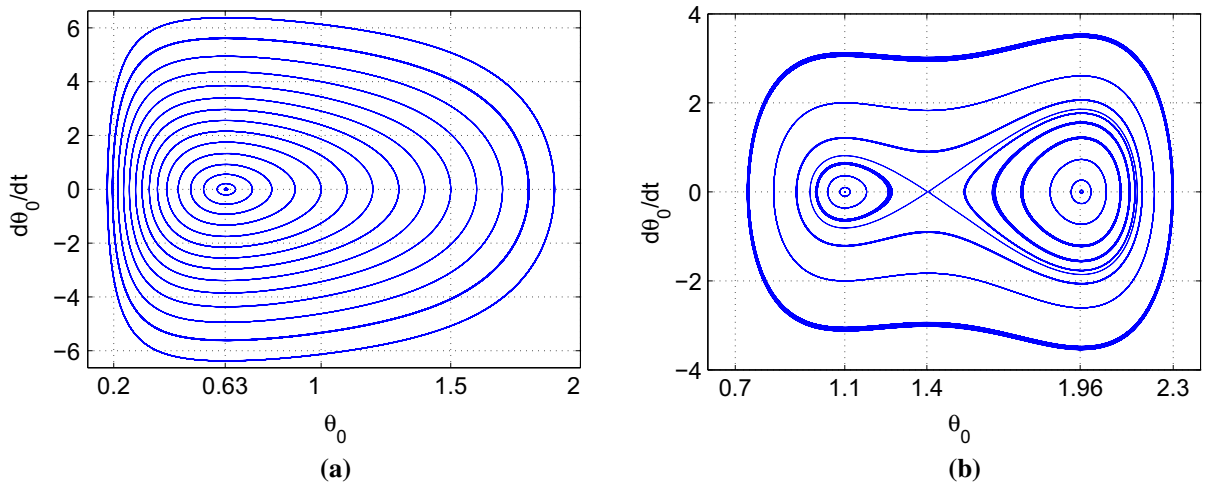

Fig. 7 Phase portrait for the θ_0 dynamics with $p_\phi = p_\psi \cos\left(\theta_0^*\right)$; $p_\psi = 9$. **a** $a = 5$, $p_\phi = 7.255$, $\theta_0^* = 0.633$. **b** $a = 11$, $p_\phi = 1.499$, $\theta_0^* = 1.403$

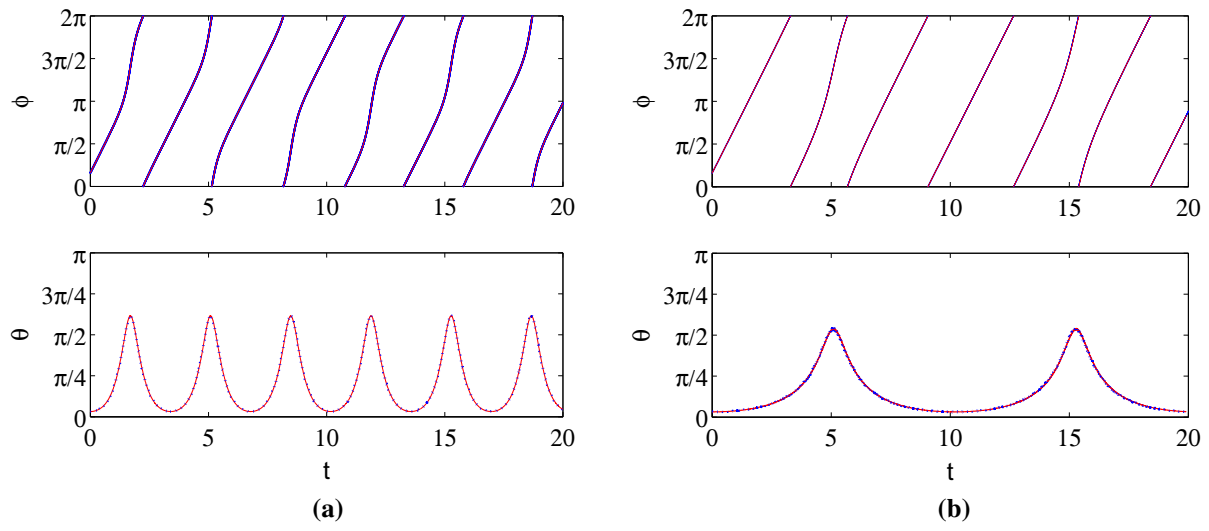

Fig. 8 As in Fig. 2, but for different values of a, $\theta\,(0)$ near 0 and $p_\psi = p_\phi = 5$. **a** $a = 1$; $\theta\,(0) = 0.0995$; $pq \equiv sn$, $e = 2$, $\alpha = -50.96$, $\beta = 50.86$, $\gamma = 37.67$, $\delta = 1.35$, $w = 2.46$, $m = 0.996$. **b** $a = 3.6$; $\theta\,(0) = 0.0982$; $pq \equiv sn$, $e = 2$, $\alpha = -0.262$, $\beta = 0.258$, $\gamma = 0.235$, $\delta = 1.11$, $w = 0.634$, $m = 0.974$. (Color figure online)

$$\ddot{\phi}\left(I_1 \sin^2\theta + I_3 \cos^2\theta\right) - 2\left(I_3 - I_1\right)\dot{\phi}\dot{\theta}\cos\theta\sin\theta$$
$$-I_3\dot{\psi}\dot{\theta}\sin\theta + I_3\ddot{\psi}\cos\theta + \mu_\phi\dot{\phi} = 0$$
$$I_3\ddot{\psi} + I_3\ddot{\phi}\cos\theta - I_3\dot{\phi}\dot{\theta}\sin\theta - \mu_\psi\dot{\psi} = 0$$

Solving the last two equations for $\ddot{\phi}$ and $\ddot{\psi}$, we obtain:

$$\ddot{\theta} = \left(1 - \frac{I_3}{I_1}\right)\dot{\phi}^2\cos\theta\sin\theta - \frac{I_3}{I_1}\dot{\psi}\dot{\phi}\sin\theta$$
$$+\frac{Md}{I_1}(g - \ddot{z})\sin\theta - \frac{\mu_\theta}{I_1}\dot{\theta}$$
$$\ddot{\phi} = \left(\frac{I_3}{I_1} - 2\right)\dot{\phi}\dot{\theta}\frac{\cos\theta}{\sin\theta} + \frac{I_3}{I_1}\frac{\dot{\psi}\dot{\theta}}{\sin\theta}$$
$$+\mu_\psi\dot{\psi}\frac{\cos\theta}{I_1\sin^2\theta} - \mu_\phi\frac{\dot{\phi}}{I_1\sin^2\theta}$$

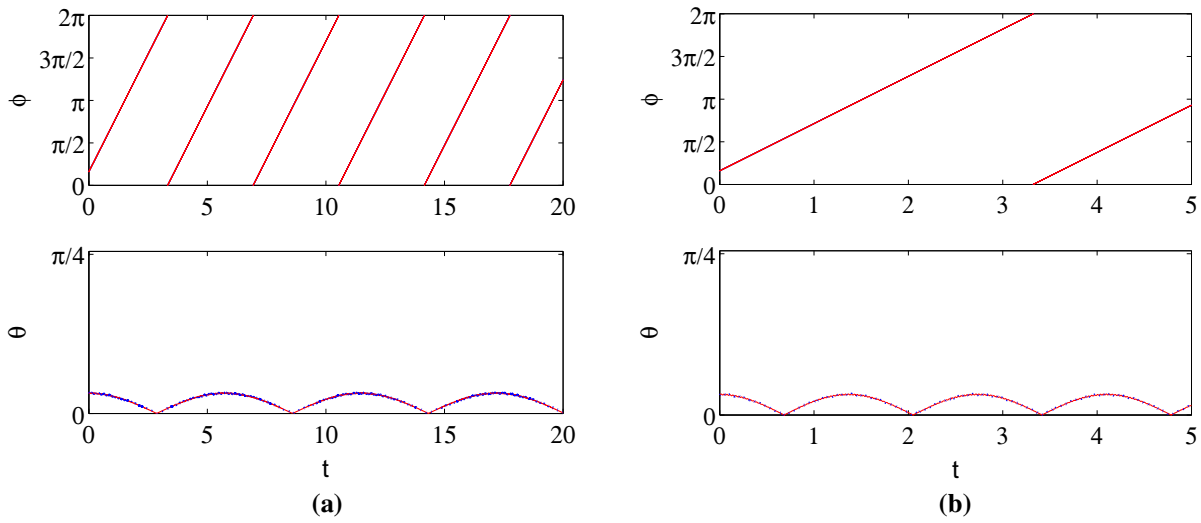

Fig. 9 As in Fig. 8. **a** $a = 3.8; \theta(0) = 0.0982$; $pq \equiv sn, e = 2, \alpha = 0.0189, \beta = 2.96 \times 10^{-4}, \gamma = 0.173, \delta = 4.99 \times 10^{-3}, w = 0.551, m = 0.024$. **b** $a = 5$; $\theta(0) = 0.0976$; $pq \equiv cn, e = 1, \alpha = -2.22 \times 10^{-5}, \beta = -6.67 \times 10^{-3}, \gamma = 2.67, \delta = 4.45 \times 10^{-3}, w = 4.596, m = 7.25 \times 10^{-7}$. (Color figure online)

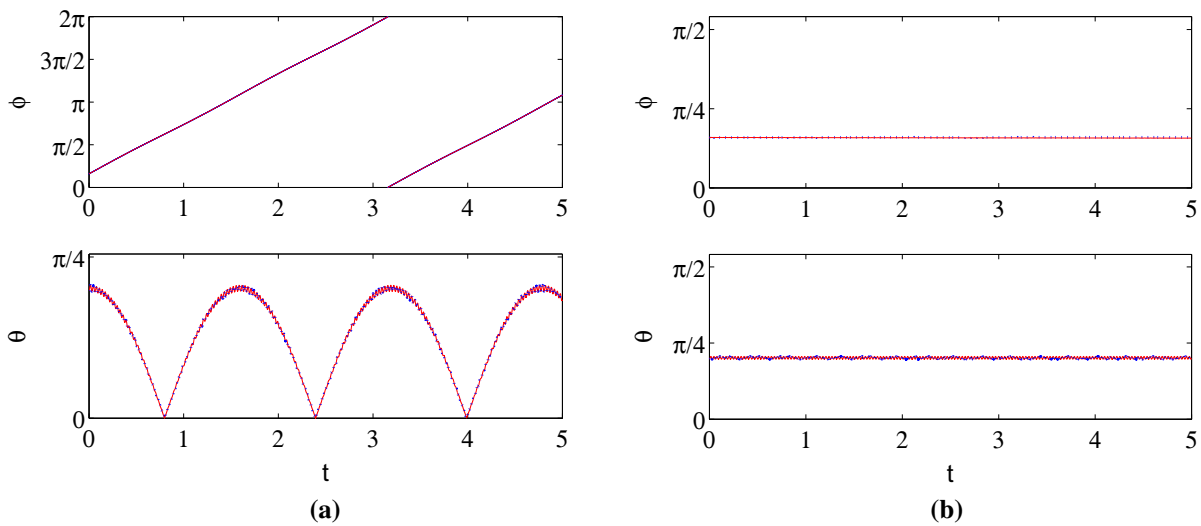

Fig. 10 As in Fig. 2, but with $\theta(0) = 0.6188, a = 5$; p_ψ and p_ϕ as specified under each figure. **a** $p_\phi = p_\psi = 5$. **b** $p_\phi = p_\psi \cos\left(\theta_0^*\right) = 4.03$. (Color figure online)

$$\ddot{\psi} = \dot{\phi}\dot{\theta}\sin\theta - \left(\frac{I_3}{I_1} - 2\right)\dot{\phi}\dot{\theta}\frac{\cos^2\theta}{\sin\theta} - \frac{I_3}{I_1}\dot{\psi}\dot{\theta}\frac{\cos\theta}{\sin\theta} - \mu_\psi\dot{\psi}\frac{\cos^2\theta}{I_1\sin^2\theta} + \mu_\phi\dot{\phi}\frac{\cos\theta}{I_1\sin^2\theta} - \frac{\mu_\psi}{I_3}\dot{\psi}$$

We can see in Fig. 11a–c that starting in the neighborhood of the "skewed sleeping top" state, the system settles onto it when friction only depends on the nutation and precession angular velocities. Figure 11d shows that the dynamics are more complex when the dissipation also depends on the spin angular velocity. We can see the system first approaching the "skewed sleeping top" state but then drifting away from it toward the upright position. Figure 12 shows that this latter

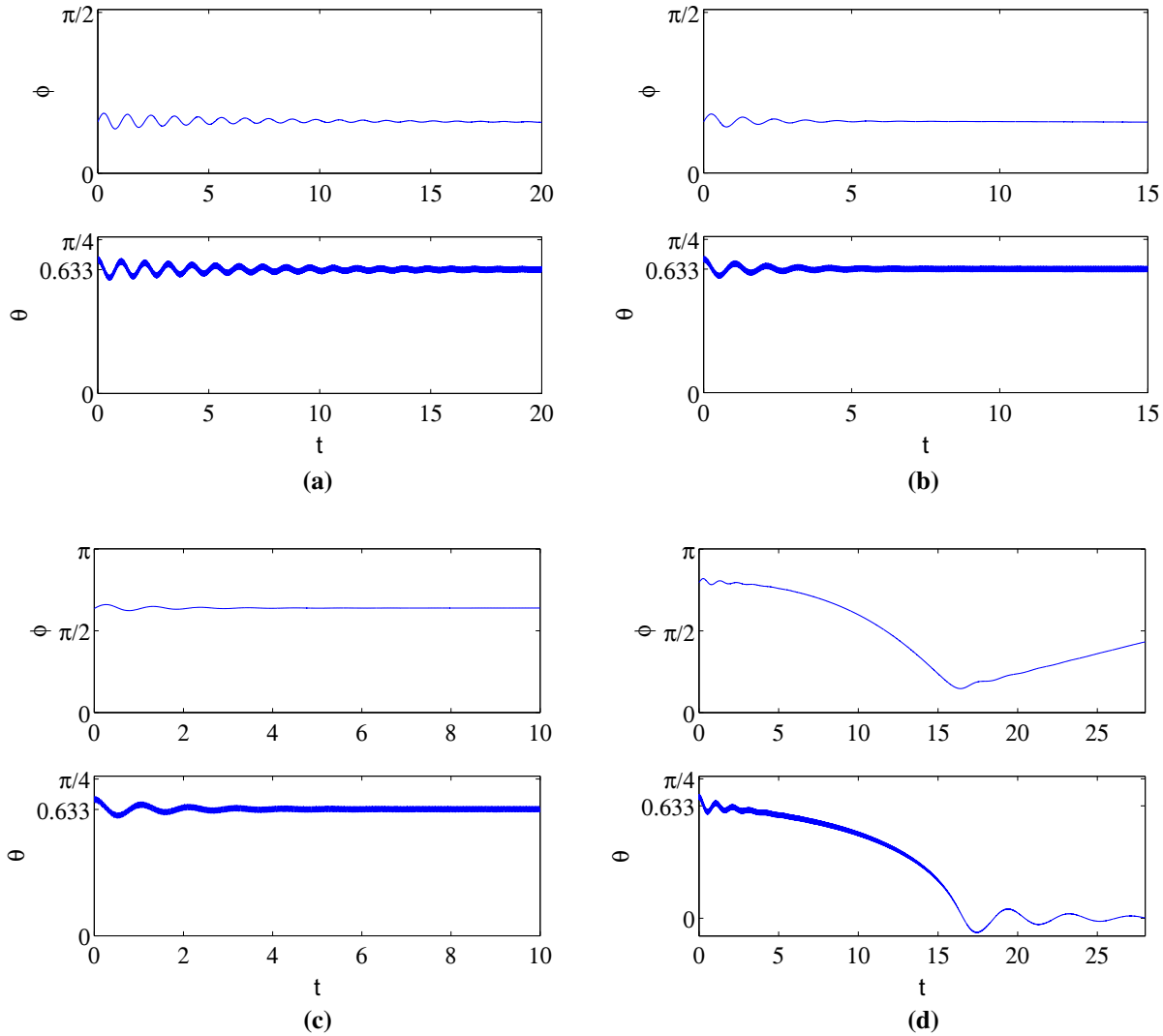

Fig. 11 Numerical integration solution for the dissipative system for different dissipation parameter values. The initial conditions used are the same as in Fig. 2b. **a** $\mu_\theta = 0.5$, $\mu_\phi = 0$, $\mu_\psi = 0$. **b** $\mu_\theta = 0$, $\mu_\phi = 0.5$, $\mu_\psi = 0$. **c** $\mu_\theta = 0.5$, $\mu_\phi = 0.5$, $\mu_\psi = 0$. **d** $\mu_\theta = 0.5$, $\mu_\phi = 0.5$, $\mu_\psi = 0.01$

behavior is due to the spin angular momentum, p_ψ, decreasing and simultaneously p_ϕ increasing such that the system approaches the upright equilibrium position which corresponds to $p_\phi = p_\psi$. This latter observation can be understood by the fact that as the top looses its spinning motion due to friction, its dynamics approach that of a pendulum under fast vertical vibration, for which the upright position is rendered stable [9]. The full study of the effects of dissipation on the dynamics is beyond the scope of this paper and will be left for future work.

5 Conclusion

In summary, we investigated the dynamics of a spinning top whose pivot point undergoes a fast vertical harmonic vibration. The method of Direct Partition of Motion was employed to reduce the non-autonomous dynamics into an autonomous second degree system governing the leading order slow nutation dynamics. Consequently, an approximate closed form solution for the full system is obtained in terms of the Jacobi elliptic functions. The analysis shows that the high-frequency

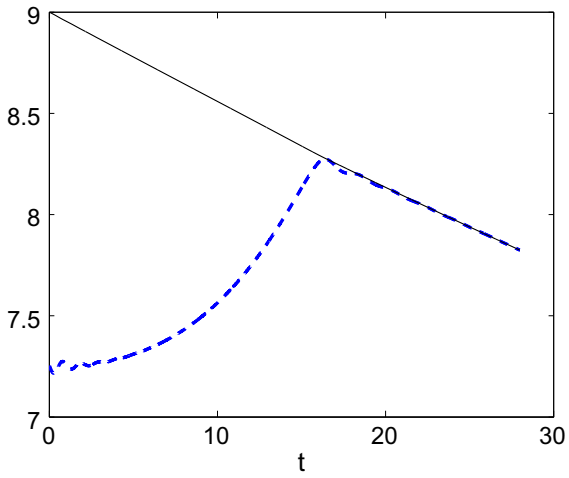

Fig. 12 The evolution of p_ϕ (*blue dotted line*) and p_ψ (*black solid line*) for the solution in Fig. 11d

excitation can stabilize the classical "sleeping top" state and the minimum required excitation amplitude is derived in terms of the physical parameters of the system. In addition, we shed light on novel non-trivial solutions that result from the high-frequency excitation, in these "skewed sleeping top" states, the spinning top is locked at a constant leading order nutation angle without any precessional motion. The results were successfully checked against the exact solution obtained from the numerical integration of the full non-autonomous system. We hope these results will encourage further investigation of the non-trivial effects of different forms of fast excitation on the dynamics of spinning rigid bodies.

References

1. Arnold, V.I.: Mathematical Methods of Classical Mechanics. Springer, Berlin (1989)
2. Blekhman, I.I.: Vibrational Mechanics-Nonlinear Dynamic Effects, General Approach, Application. World Scientific, Singapore (2000)
3. Ge, Z.M., et al.: The regular and chaotic motions of a symmetric heavy gyroscope with harmonic excitation. J. Sound Vib. **198**(2), 131–147 (1996)
4. Goldstein, H., et al.: Classical Mechanics. Addison Wesley, San Francisco (2002)
5. Jensen, J.S.: Non-trivial effects of fast harmonic excitation. Ph.D. dissertation, DCAMM Report, S83. Dept. Solid Mechanics, Technical University of Denmark (1999)
6. Lawerance, A.: Modern Inertial Technologies: Navigation, Guidance and Control. Springer, New York (1992)
7. Martin Sanchez, A., et al.: Solution of the anharmonic quartic potential oscillator problem. J. Sound Vib. **161**(1), 19–31 (1993)
8. Rimrott, F.P.J.: Introductory Attitude Dynamics. Springer, New York (1989)
9. Stephenson, A.: XX. On induced stability. In: Philosophical Magazine Series 6, **15**(86), 233–236 (1908)
10. Thomsen, J.J.: Vibrations and Stability, Advanced Theory, Analysis and Tools. Springer, Berlin (2003)
11. Thomsen, J.J.: Slow high-frequency effects in mechanics: problems, solutions, potentials. Int. J. Bifurc. Chaos **15**, 2799–2818 (2005)
12. Townsend, N., Shenoi, A.: A gyroscopic wave energy recovery system for marine vessels. IEEE J. Ocean. Eng. **37**(2), 271–280 (2012)